

FRACTAL STRUCTURE AND PHASE TRANSITIONS AT HIGH ENERGIES¹M. Blažek²*Institute of Physics, Slovak Academy of Sciences, 842 28 Bratislava, Slovakia*

Received 2 February 1994, accepted 28 February 1994

In the present contribution our approaching the quark-gluon plasma phase transition is analysed by means of the sufficiently extended fundamental equation describing self-similar processes. The presence of that kind of processes is usually inferred from non-vanishing scaling indices characterizing intermittency (à la Bialas and Peschanski) or the G-moments (à la Hwa and Pan). We give a relation between those two sets of scaling indices thereby arguing that (under certain assumptions) the information involved in one set is contained also in the other one. Several suggestions to experimental groups are formulated, too. Special attention is paid to the antiproton-proton collisions at $\sqrt{s} = 1.8$ TeV and (16)oxygen colliding with emulsion nuclei at 60, 200 (and higher) A GeV.

1. Introduction

High energy collisions lead to production of many secondaries. It is expected that nearness to the phase transition (say, into quark-gluon plasma) will be reflected also into multiplicity distributions. On the other hand, there are several cases where the multiparticle production reveals multifractality [1]. And multifractal structure can be interpreted in terms of the self-similar processes. Therefore a natural question arises, namely, whether -or to what extent- the multifractality itself or the underlying self-similar processes can be considered as a signature for identifying the presence of (or the "distance" from) the phase transition.

In the next Section global properties of self-similar processes are mentioned; we discuss there also an extended version of the fundamental equation which incorporates them in a natural way. In the third Section this equation is applied to the data on antiproton-proton collisions at $\sqrt{s} = 1.8$ TeV as well as on the $^{16}\text{O} + \text{Ag}/\text{Br}$ collisions at 60 and 200 A GeV. We show there that with further assumptions (expressing mostly the simplest possibilities) the present approach is able to specify the location of the phase transition (or to guess at least the lower limit, in the energy scale) where it can be expected.

¹Presented at School and Workshop on Heavy Ion Collisions, Bratislava, 13-18 September 1993

²E-mail address: BLAZEK@SAVBA.SK

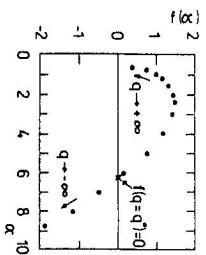


Figure 1. A concrete spectral function which clearly exhibits the fact that the corresponding density of singularities vanishes at a finite value of the order q . The points are taken from [10] and they characterize a growth-site probability distribution.

In high energy physics presence of self-similar processes is usually ascribed to the appearance of non-vanishing scaling indices which characterize on one hand the intermittency [2] and on the other one the multifractality specified by the G-moments, [3]. Relations between those two sets of scaling indices are formulated in the fourth Section; they involve also the corresponding intercepts as well as an effective average multiplicity, N_0 . All those quantities are accessible by the experimental groups without additional complications and we propose to publish them together with the scaling indices as more complete characteristics of multifractal phenomena. In the last Section we shortly conclude that the knowledge of all those quantities will eventually allow us to verify (i) the presence of global properties specifying the self-similar processes, (ii) the mutual dependence of both sets of scaling indices mentioned above, and (iii) to estimate, in a more accurate way, the distance from the phase transition.

2. Global properties of self-similar processes

2.1 Preliminaries

Let us concentrate on the probability flow through a (pseudo)rapidity window ΔY (of the size $= 1$). We assume that in the first step the window ΔY is partitioned into C_j portions of length l_j and with the corresponding probability flow (or, more correctly, frequency numbers) p_j where $j = 1, 2, \dots, K$. Moreover, we admit that there is a portion of the length Δl where no probability flows at all. Then the following two normalization constraints should be satisfied,

$$\sum_{j=1}^K C_j l_j + \Delta l = 1, \quad (2.1)$$

$$\sum_{j=1}^K C_j p_j = 1. \quad (2.2)$$

If

$$\Delta l \neq 0 \quad (2.3)$$

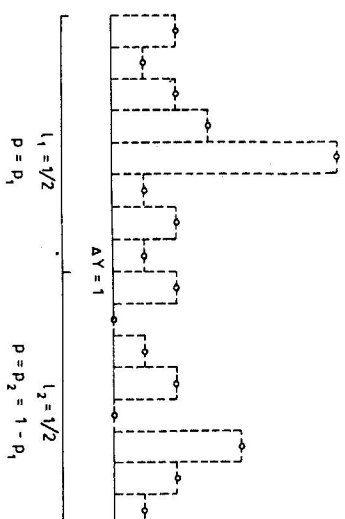


Figure 2. Schematic partitioning of the "(pseudo)rapidity" variable.

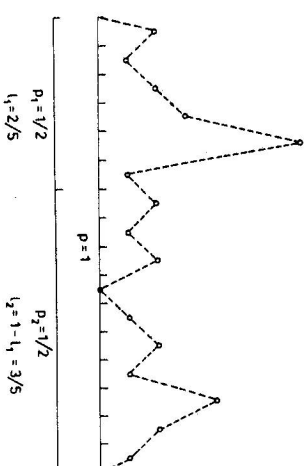


Figure 3. Schematic partitioning of the "probability" variable.

we say that the empty bin effect is present there; in general,

$$0 \leq \Delta l < 1. \quad (2.4)$$

If at least one of the coefficients C_j is larger than unity we say that the multiple bin phenomenon is present there (compare [4]).

The presence of self-similarity induces validity of the following fundamental equation [5], [6],

$$\sum_{j=1}^K C_j p_j^q / l_j^q = 1. \quad (2.5)$$

The quantity $\tau = \tau(q)$ represents scaling indices which characterize multifractality in terms of the G-moments, [3],

$$G_q = \sum_{i=1}^M \left(\frac{n_i}{N} \right)^q \Theta(n_i - q), \quad (2.6)$$

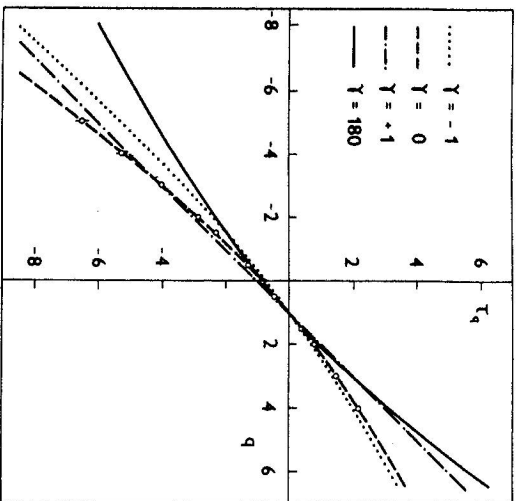


Figure 4. Scaling function, $\tau = \tau(q, \gamma)$ characterizing the antiproton-proton collisions at $\sqrt{s} = 1.8$ TeV, for four values of the mixing angle γ .

namely,

$$\langle G_q \rangle \propto g_q M^{-\tau_q}. \quad (2.7)$$

In (2.6), n_i expresses the number of particles observed in the i -th bin, M gives the number of bins, $N = \sum_i n_i$ being the total number of particles observed in one event under consideration and $\Theta(x)$ is the step function which is equal to 1 if $x \geq 0$ and zero if $x < 0$. The angular brackets in (2.7) (and in the following part of the present contribution) express averaging over events and g_q are the intercepts corresponding to the scaling indices $\tau(q)$.

The intermittency is usually introduced by means of the requirement that the factorial moments F_q ,

$$F_q = M^{q-1} \sum_{i=1}^M [E_q(n_i)] / N^q \quad (2.8)$$

with

$$E_q(n) = n(n-1)\dots(n-q+1) \equiv E \quad (2.9)$$

reveal the power-law dependence (compare [2]),

$$\langle F_q \rangle \propto f_q M^{\alpha_q} \quad (2.10)$$

in some range of the numbers M ; f_q denote the intercepts corresponding to the scaling indices α_q . As far as the multiplicities involved are sufficiently large, rel. (2.7) and

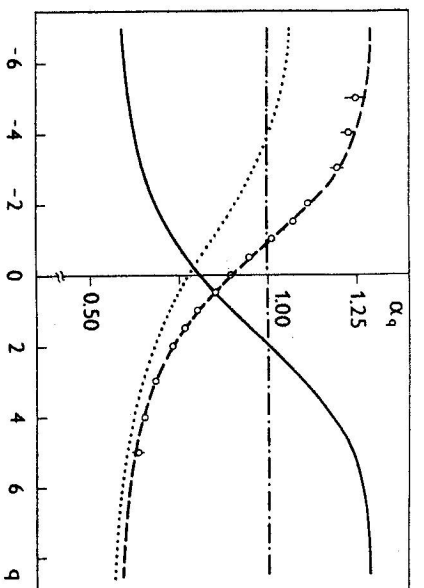


Figure 5. Strength of singularities, $\alpha = \alpha(q, \gamma)$; otherwise the same as in Fig. 4.

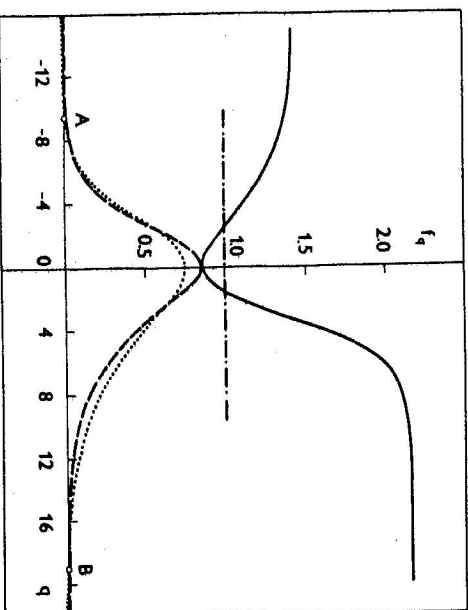


Figure 6. Density of singularities, $f = f(q, \gamma)$. The points A and B mark the location where the density $f(q, \gamma = -1)$ vanishes; otherwise the same as in Fig. 4

(2.10) give

$$\alpha_q = q - 1 - \tau_q. \quad (2.11)$$

Modification of rel. (2.11) due to the presence of finite multiplicities is considered in the fourth Section of the present contribution.

Besides scaling indices also the strength $\alpha = \alpha(q) = d\tau/dq$ and the density $f = f(q) = q\alpha - \tau$ of the underlying singularities as well as the spectral function $f = f(\alpha)$ characterize a fractal structure. It is worthwhile to note that the fundamental equation (2.5) induces convex property of the scaling function $\tau = \tau(q)$ and of the

spectral function $f = f(\alpha)$, i.e. $d^2\tau/dq^2 < 0$ (compare [5]). Moreover, the density $f \equiv f(q)$ is a non-vanishing function for any finite order q of the statistical moment under consideration (compare [4]).

Scaling function $\tau = \tau(q)$ enters also the definition of generalized (Benyi) dimensions $D = D(q)$,

$$D(q) = \tau(q)/(q-1). \quad (2.12)$$

Let us add that the case when D is independent (at least to a required degree of accuracy) of the order q can be considered as a signature for the presence of the (thermal) phase transition [1], [7], [8].

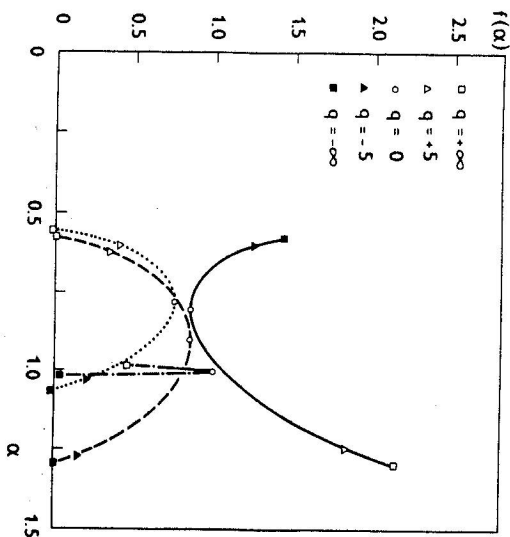


Figure 7. Spectral function, $f = f(\alpha, \gamma)$. There are clearly seen the points where the density $f = f(q, \gamma = -1)$ vanishes; otherwise the same as in Fig. 4.

2.2 Extended fundamental equation

There are serious indications (some of them are quoted e.g. in [6], [9]) that in some cases the scaling function as well as the spectral function are concave functions of their argument and the density $f \equiv f(q)$ vanishes at some finite value(s) of the order q . Let us demonstrate at least the last fact in Fig. 1 where the results [10] of a growth-site probability distribution are seen (theoreticians should not disregard such facts as far as they should follow a scientific attitude...; compare [11]).

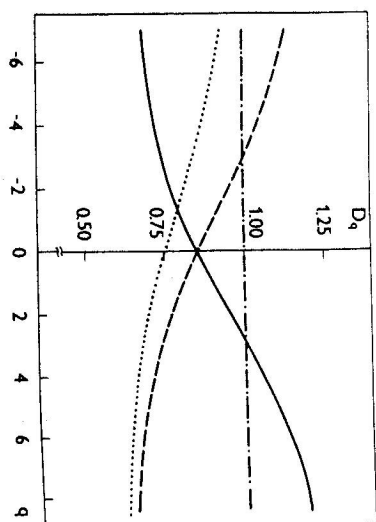


Figure 8. Generalized dimension, $D = D(q, \gamma)$; otherwise the same as in Fig. 4.

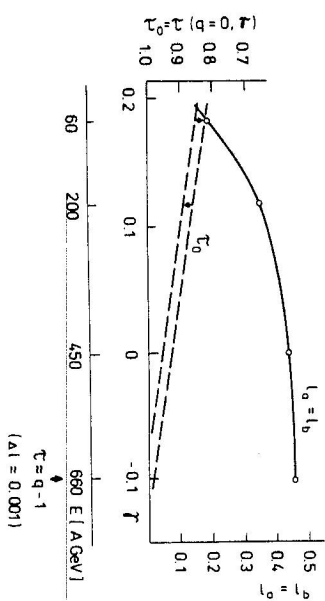


Figure 9. Linear approximation of the energy dependence of mixing angle $\gamma = \gamma(E)$ and of the scaling index $\tau_0 = \tau_0(q = 0, \gamma = \gamma(E))$ allowing to deduce the location (or at least the lower bound) where the (thermal) phase transition can be expected. Experimental values at $E = 60$ and 200 A GeV on $^{16}\text{O} + \text{Ae}/\text{Br}$ collisions are taken from [14].

Let us express the extended fundamental equation incorporating the aforementioned cases, in the following form,

$$\sum_{j=1}^K C_j p_j^q / I_j^q = 1 \quad (2.13)$$

where

$$\hat{q} - \hat{q}^* = (q - q_q^*) \cos \gamma + (\tau - \tau_q^*) \sin \gamma, \quad (2.14)$$

$$\hat{\tau} - \hat{\tau}^* = -(q - q_q^*) \sin \gamma + (\tau - \tau_q^*) \cos \gamma$$

with γ being mixing angle. The quantities with asterisk represent corresponding translations; their value is determined by the requirement that, on one hand eq.(2.13) with $\gamma = 0$ should reduce to eq.(2.5) and, on the other hand, with $\gamma = \pi$ to

$$\sum_{j=1}^K C_j I_j^{-\tau_0} / I_j^{q-1} = 1. \quad (2.15)$$

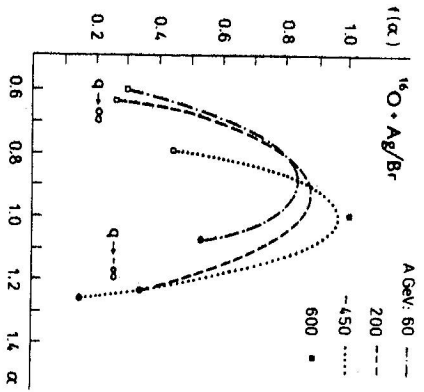


Figure 10. Spectral function, $f = f(\alpha, \gamma)$ characterizing $^{16}\text{O} + \text{Ag}/\text{Br}$ collisions.

Then $\hat{q}^* = q_q^* = \frac{1}{2}$ and $\hat{\tau}^* = \hat{\tau}_\tau^* = \frac{1}{2}\tau_0$ where

$$\tau_0 = \tau(q = 0, \gamma). \quad (2.16)$$

In this case the transformation (2.14) can be expressed in the form

$$\begin{aligned} \hat{q} &= q \cos \gamma + \tau \sin \gamma + \mu, \\ \hat{\tau} &= -q \sin \gamma + \tau \cos \gamma + \nu \end{aligned} \quad (2.17)$$

and

$$\begin{aligned} \mu &= \frac{1}{2}(1 - \cos \gamma) - \tau_q^* \sin \gamma, \\ \nu &= \frac{1}{2}\tau_0(1 - \cos \gamma) + q_\tau^* \sin \gamma. \end{aligned} \quad (2.18)$$

Let us recall that eq.(2.5) describes self-similar processes characterizing fractal structure of probability flow through the bin sizes arising by successive partitioning of, say, the (pseudo)rapidity, compare Fig.2. On the other hand, eq.(2.15) allows a complementary interpretation, namely: it describes self-similar processes characterizing the fractal structure in (pseudo)rapidity when the successive partitioning is performed in the probability variable, [6], [9], compare Fig.3. We suggest to verify this complementary approach and consequences which follow from its application; two attempts to do it are presented in the following Section.

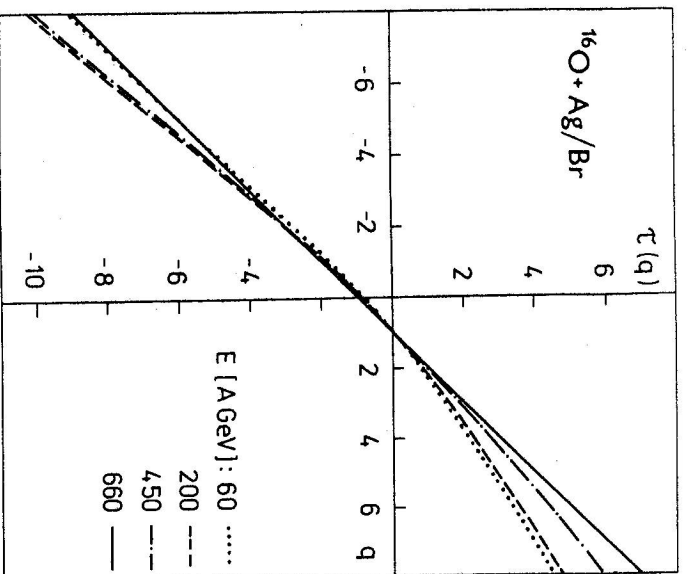


Figure 11. Scaling function $\tau = \tau(q, \gamma)$ characterizing $^{16}\text{O} + \text{Ag}/\text{Br}$ collisions; the value $\gamma = -0.1$ (i.e. E about 660 GeV) corresponds to the (possible) thermal phase transition.

In the extended case also the following generalized dimension can be considered as a convenient characterization of the underlying fractal structure,

$$D = D_\tau = q/(\tau - \tau_0) \quad (2.19)$$

τ_0 being given by (2.16).

3. Applications of the extended fundamental equation (2.13)

In what follows two cases are considered, namely, when in (2.18),

$$q_\tau^* = 1, \quad \tau_q^* = 0 \quad (3.1)$$

and

$$q_q^* = \frac{1}{2}, \quad \tau_q^* = \frac{1}{2}\tau_0. \quad (3.2)$$

In the next analyses the extended fundamental equation (2.13) is considered with two kinds of bin sizes (i.e. $K = 2$) and it is solved together with both constraints (2.1) and (2.2).

3.1 Antiproton-proton collisions at $\sqrt{s} = 1.8$ TeV

It turns out that in this case the possibility (3.1) represents a more instructive approach. Especially, Table 1 shows the (preliminary) experimental values of the scaling indices $\tau(q)$, [12], as well as theoretical output which arrives by solving eq.(2.5) (i.e. eq.(2.13) with $\gamma = 0$). As it is seen, the agreement between those two kinds of data is quite sufficient. The value of $\tau_0 = \tau(q = 0, \gamma = 0) = -0.8513$ is taken from the experimental source [12]. Due to the fact that $\tau_0 \neq -1$ the empty bin effect is present there, however, the multiple bin phenomenon is nearly absent there (since $C_1 \approx C_2 \approx 1$).

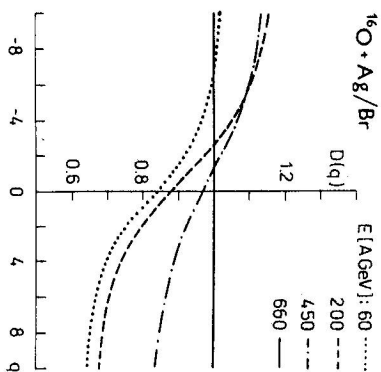


Figure 12. Generalized dimension, $D = D(q, \gamma)$, rel.(2.12) characterizing $^{16}\text{O} + \text{Ag/Br}$ collisions; $D = D(q, \gamma = -0.1)$ corresponds to the (possible) thermal phase transition.

The remaining three parameters are fixed at the following value,

$$p_1 = 0.526, \quad (3.3)$$

and

$$l_1 = 0.3291, \Delta l = 0.1088. \quad (3.4)$$

Theoretical curve $\tau = \tau(q, \gamma = 0)$ is seen in Figure 4. The same Figure presents also three other solutions of eq.(2.13), $\tau = \tau(q, \gamma)$, namely for $\gamma = -1, 1, 180$, respectively. In all three cases the same value of p_1 is taken as in rel.(3.3) (thereby simulating the antiproton-proton case). However, the value of $\tau_0 = \tau(q = 0, \gamma)$ for corresponding three cases as well as the value of l_1 and Δl are tuned up so that the constraints (2.1), (2.2) and $\tau(q = 1) = 0$ be satisfied to the required degree of accuracy. Numerical value of those parameters is presented in Table 2. Let us note that for instance the natural requirement for the size of the empty bins, Δl , expressed by rel.(2.4), prevents sometimes the mixing angle γ from taking on some real values.

The strength $\alpha = \alpha(q, \gamma)$, density $f = f(q, \gamma)$, spectral function $f = f(\alpha, \gamma)$ and generalized dimensions $D = D(q, \gamma)$ (with $\gamma = -1, 0, 1, 180$) are seen in Figures 5, 6, 7 and 8, respectively. Especially the last Figure suggests that $D(q, \gamma \approx +1)$ is nearly independent of q thereby indicating possible presence of (thermal) phase transition (some more details are included into the next part of this Section). Let us add that Figure 6 clearly exhibits the possible vanishing of the density $f = f(q)$ and thereby indicating, in this approach, the possible appearance of the so called non-thermal phase transition, [13] (and also Fig.1).

Table 1. Experimental, $(\tau_q)_{\text{exper}}$, and theoretical, $(\tau_q)_{\text{theor}}$, values of the scaling indices $\tau = \tau(q)$ obtained in the antiproton-proton collisions at $\sqrt{s} = 1.8$ TeV. The experimental values are taken from [12]; the theoretical values are obtained by solving eq.(2.13) of the present paper (where $K = 2$, $\gamma = 0$ and applying (3.1); other parameters are specified by $\gamma = 0$ in Table 2).

$\bar{p}p$ collisions at $\sqrt{s} = 1.8$ TeV			
q	$(\tau_q)_{\text{exper}}$	$(\tau_q)_{\text{theor}}$	
-5	-6.508 ± 0.039	-6.511	
-4	-5.273 ± 0.031	-5.251	
-3	-4.054 ± 0.022	-4.029	
-2	-2.878 ± 0.014	-2.871	
-0.5	-1.311 ± 0.002	-1.312	
0	-0.8513 ± 0.003	-0.852	
0.5	-0.415 ± 0.001	-0.414	
2	0.766 ± 0.003	0.768	
3	1.470 ± 0.007	1.476	
4	2.138 ± 0.010	2.141	
5	2.784 ± 0.014	2.776	

Table 2. Value of parameters entering eq.(2.13) for four values of the mixing angle γ . The value of τ_0 at $\gamma = 0$ is taken from experimental data, [12]. In all four cases value of the parameter p_1 is fixed at 0.526.

$\bar{p}p$ collisions at $\sqrt{s} = 1.8$ TeV				
γ	-1	0	+1	180
τ_0	-0.750	-0.8513	-1	-0.8513
l_1	0.560	0.3291	0.5200	0.3291
Δl	0.168	0.1088	0.0243	0.1088

Table 3. Value of the scaling indices characterizing fractal structure which arises in the (16) oxygen-emulsion nuclei collisions at 60 A GeV. The experimental data are taken from [14] and the theoretical values come by solving eq.(2.13) with (3.2).

$^{16}\text{O} + \text{Ag/Br}$ at 60 A GeV			
q	$(\tau_q)_{\text{exper}}$	$(\tau_q)_{\text{theor}}$	$\left[\frac{(\tau_q)_{\text{exper}} - (\tau_q)_{\text{theor}}}{(\Delta\tau_q)_{\text{exper}}}\right]^2$
-6	-6.953 ± 0.353	-6.942	9.71×10^{-4}
-5	-5.887 ± 0.281	-5.879	8.11×10^{-4}
-4	-4.821 ± 0.211	-4.820	2.25×10^{-5}
-3	-3.764 ± 0.144	-3.772	3.09×10^{-3}
-2	-2.734 ± 0.085	-2.746	1.92×10^{-2}
-1	-1.752 ± 0.041	-1.759	2.91×10^{-2}
0	-0.836 ± 0.015	-0.836	0
2	0.756 ± 0.012	0.757	2.78×10^{-2}
3	1.446 ± 0.024	1.445	1.74×10^{-3}
4	2.096 ± 0.036	2.039	6.94×10^{-3}
5	2.721 ± 0.048	2.719	1.74×10^{-3}
6	3.330 ± 0.060	3.334	4.44×10^{-3}

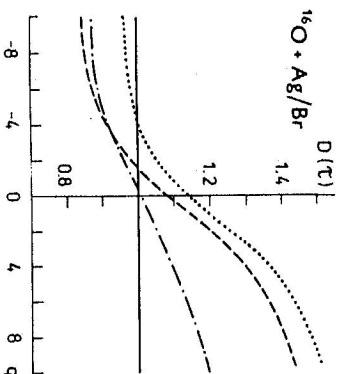


Figure 13. Generalized dimension, $D = D(q, \gamma)$, rel.(2.19), characterizing $^{16}\text{O} + \text{Ag/Br}$ collisions; notation is the same as in Fig.12.

3.2 Oxygen-emulsion nuclei collisions

Experimental data [14] on multifractal structure observed in oxygen-emulsion nuclei collisions at 60 and 200 A GeV represent, so far, a unique way to draw special conclusions about the possible phase transition into quark-gluon plasma. The reason for this standpoint arrives from the fact that those two sets of data obtained at different energies are quite rich and they are elaborated, essentially, by the same techniques. In our approach it is mainly the energy dependence of the mixing angle γ which we are looking for.

Table 4. The same as Table 3, but now at 200 A GeV.

$^{16}\text{O} + \text{Ag/Br}$ at 200 A GeV			
q	$(\tau_q)_{\text{exper}}$	$(\tau_q)_{\text{theor}}$	$\left[\frac{(\tau_q)_{\text{exper}} - (\tau_q)_{\text{theor}}}{(\Delta\tau_q)_{\text{exper}}}\right]^2$
-6	-7.678 ± 0.236	-7.704	1.21×10^{-2}
-5	-6.470 ± 0.187	-6.467	2.57×10^{-4}
-4	-5.265 ± 0.141	-5.248	1.45×10^{-2}
-3	-4.074 ± 0.097	-4.058	2.72×10^{-2}
-2	-2.922 ± 0.059	-2.917	7.18×10^{-3}
-1	-1.848 ± 0.030	-1.849	1.11×10^{-3}
0	-0.874 ± 0.012	-0.874	0
2	0.790 ± 0.010	0.791	1.00×10^{-2}
3	1.518 ± 0.020	1.517	2.50×10^{-3}
4	2.205 ± 0.030	2.203	4.44×10^{-3}
5	2.867 ± 0.041	2.864	5.35×10^{-3}
6	3.513 ± 0.051	3.512	3.84×10^{-4}

Let us start with eq.(2.13). Applying the second possibility (3.2) we express rel.(2.18) in the form,

$$\mu = \frac{1}{2}(1 - \cos \gamma) - \frac{1}{2}\tau_0 \sin \gamma, \quad \nu = \frac{1}{2}\tau_0(1 - \cos \gamma) + \frac{1}{2}\sin \gamma. \quad (3.5)$$

Now, it is convenient to reformulate eq.(2.17) with (3.5) in terms of the asymptotics

$$\tau_+ \equiv \tau(q \gg 1) = q\alpha_+ - f_+ \quad \text{and} \quad \tau_- \equiv \tau(q \ll -1) = q\alpha_- - f_- \quad (3.6)$$

(more details in [9]). Experimental value of the scaling indices $\tau(q)$ shown in Tables 3 and 4 allow to deduce the numerical guess of the asymptotics as it is seen in Table 5 (the value of τ_0 is taken from experimental data). This asymptotics considered as input in the reformulated eq.(2.17) with (3.5) leads to the output as it is seen in Table 6 (without any free parameter). Then eq.(2.13) gives the theoretical values of the scaling indices as they are presented in Tables 3 and 4 (compare [15]). The nice agreement between experimental and theoretical values of the scaling indices (as it is indicated by last columns in Tables 3 and 4) stimulates our attempt to extrapolate, even if very tentatively, the energy dependence of the mixing angle $\gamma = \gamma(E)$ and the value $\tau_0 = \tau_0(E)$ where $\tau_0 = \tau(q = 0, \gamma)$ with $\gamma' = \gamma$ at the energy $E = 60$ and 200 A GeV. Assuming a linear (i.e. the most simple) dependence we arrive to the result (compare Fig. 9) that at the energy $E \approx 660$ A GeV, with good approximation

$$\tau(q) = q - 1 \quad (3.7)$$

(and $\tau(0) = -1$); this means,

$$D(q) = 1, \quad (3.8)$$

independently of the order q . Then $\Delta l \approx 0.001$ and $\gamma \approx -0.1$. As far as (3.7) is satisfied, we obtain $\alpha(q) = 1$ and $f(\alpha) = q\alpha - (q - 1) = 1$ (for all q 's): the spectral function is shrunk into one point. Moreover at $E \approx 450$ A GeV our analysis gives $\gamma \approx 0$ and $\tau(q = 0, \gamma = 0) = -0.969$. The spectral function $f = f(\alpha)$ for corresponding four energies is seen in Fig. 10. The scaling indices $\tau = \tau(q, \gamma)$ and the generalized dimensions $D = D(q, \gamma)$ rel.(2.12), and $D = D(\tau(q), \gamma)$ rel.(2.19) for $\gamma = \gamma(E)$, $E = 60, 200, 450$ and 660 A GeV are seen in Figures 11, 12 and 13, respectively. Table 7 gives the numerical value of the scaling indices $\tau = \tau(q, \gamma(E))$ for $E = 450$ which can be considered as our prediction.

We conclude that as far as the assumptions involved in the present contribution are acceptable, the phase transition in $^{16}\text{O} + \text{Ag}/\text{Br}$ collisions should not appear at the energies which are lower than about 660 A GeV.

Table 5. Value of the input data involved in solution of the extended fundamental equation (2.17) with (3.5) reformulated in terms of the asymptotics τ_+ and τ_- , rel.(3.6), completed by the condition that all bins are of the same size (i.e. $l_1 = l_2$).

$^{16}\text{O} + \text{Ag}/\text{Br}$			
	at 60 A GeV	at 200 A GeV	
α_+	0.605	0.632	
f_+	0.287	0.266	
α_-	1.068	1.256	
f_-	0.530	0.145	

4. Relations between two sets of scaling indices

In high energy physics the multifractal structure is usually characterized in terms of the scaling indices $\tau = \tau(q)$ and $a = a(q)$ introduced by (2.7) and (2.10), respectively. We shall show that those two kinds of scaling indices are related as far as they are deduced from the same set of events (and other, kinematical, characteristics being also the same). This fact allows to conclude that, in principle, it is sufficient to deal only with one set of those scaling indices. We sketch briefly a procedure which allows to establish the corresponding relations.

Table 6. Value of the output data specifying the parameters which enter the extended fundamental equation (2.13).

$^{16}\text{O} + \text{Ag}/\text{Br}$			
	at 60 A GeV	at 200 A GeV	
γ	1.817×10^{-1}	1.172×10^{-1}	
Δl	2.434×10^{-1}	1.246×10^{-1}	
$l_1 = l_2$	1.876×10^{-1}	3.528×10^{-1}	
C_1	1.613×10^0	1.318×10^0	
C_2	2.420×10^0	1.163×10^0	
p_1	3.660×10^{-1}	5.190×10^{-1}	
p_2	1.693×10^{-1}	2.717×10^{-1}	

Table 7. Predicted value of the scaling indices $\tau = \tau(q)$ characterizing multifractality in $^{16}\text{O} + \text{Ag}/\text{Br}$ collisions at 450 GeV.

$^{16}\text{O} + \text{Ag}/\text{Br}$ at 450 A GeV		
q	$(\tau_q)_{theor}$	
-6	-7.681	
-5	-6.482	
-4	-5.306	
-3	-4.160	
-2	-3.051	
-1	-1.987	
0	-0.969	
2	0.925	
3	1.810	
4	2.664	
5	3.494	
6	4.306	

First of all let us express the function $E = E_q(n)$, rel.(2.9), in the form $E = [\Gamma(n+1)]/\Gamma(n-t)$ and $n+1 = n(1+1/n)$, $n-t = n(1-t/n)$ with

$$t = q - 1. \quad (4.1)$$

Applying the Stirling' asymptotics for Γ -functions and multiplying all corresponding series expansions we obtain

$$E = n^q \sum_{k=0}^{\infty} \frac{A_k(q)}{n^k} \quad (4.2)$$

where, bearing in mind rel.(4.1),

$$A_0(q) = 1,$$

$$A_1(q) = -\frac{1}{2}t(t+1),$$

$$A_2(q) = \frac{1}{24}t(3t^3 + 2t^2 - 3t - 2),$$

$$A_3(q) = \frac{1}{48}t^2(-t^4 + t^3 + 3t^2 - t - 2),$$

$$A_4(q) = \frac{1}{2}t\left(\frac{t^7}{192} - \frac{t^6}{48} - \frac{t^5}{288} + \frac{t^4}{15} - \frac{5t^3}{576} - \frac{t^2}{16} + \frac{t}{144} + \frac{1}{60}\right), \quad (4.3)$$

etc. With respect to (4.2) the factorial moments (2.8) acquire the form

$$F_q = M^{q-1} \sum_{i=1}^M \left[\left(\frac{n_i}{N}\right)^q + \frac{1}{N} \left(\frac{n_i}{N}\right)^{q-1} A_1(q) + \frac{1}{N^2} \left(\frac{n_i}{N}\right)^{q-2} A_2(q) + \dots \right] \quad (4.4)$$

or applying rel.(2.6),

$$F_q M^{1-q} = G_q + \frac{1}{N} G_{q-1} A_1(q) + \frac{1}{N^2} G_{q-2} A_2(q) + \dots \quad (4.5)$$

Averaging over events leads to the relation,

$$\langle F_q \rangle M^{1-q} = \langle G_q \rangle + \langle N^{-1} G_{q-1} \rangle A_1(q) + \langle N^{-2} G_{q-2} \rangle A_2(q) + \dots \quad (4.6)$$

To proceed further we assume that besides rel.(2.7) and (2.10) appearance of the fractal structure is characterized also by an effective average multiplicity N_0 satisfying relation

$$\langle N^{-\lambda} G_q \rangle \propto N_0^{-\lambda} g_q \times M^{-\tau_q} \quad (4.7)$$

with $\lambda = 0, 1, 2, \dots$; the intercepts g_q can be determined when $\lambda = 0$. Let us add that rel.(4.7) generalizes relation (2.7). Now, rel.(4.5) together with (2.7), (2.10) and (4.7) lead to the following fundamental relation,

$$f_q M^{q-q+1} = g_q M^{-\tau_q} + g_{q-1} M^{-\tau_{q-1}} \frac{A_1(q)}{N_0} + g_{q-2} M^{-\tau_{q-2}} \frac{A_2(q)}{N_0^2} + \dots \quad (4.8)$$

(4.8) It is seen that especially with large value of the effective average multiplicity N_0 rel.(4.8) gives an approximate equality between the corresponding slopes in the well known form (2.11), $a_q = q - 1 - \tau_q$. On the other hand, rel.(4.8) allows to express e.g. the first term on its r.h.s. in terms of the scaling indices a_q , the corresponding slopes f_q and the average multiplicity N_0 (more details will be published elsewhere).

5. Conclusions

In this paper the multifractal structure observed in antiproton-proton collisions at $\sqrt{s} = 1.8$ TeV as well as in the oxygen-emulsion nuclei collisions at 60 and 200 A GeV are described in terms of the extended fundamental equation characterizing the self-similar processes. In both cases the empty bin effect and in the second case also the multiple bin phenomenon are observed. Moreover, simple assumptions especially about energy dependence of the mixing angle γ and the value of the scaling index $\tau = \tau(q=0)$ (specifying essentially the global properties of the underlying self-similar processes) in the second case help to predict the behaviour of scaling indices (as well as of other characteristics) at higher energies. As a concrete consequence we arrive to the conclusion that in this case the energy E about 660 A GeV represents the lower limit for the possible quark-gluon plasma formation. This direction of our work allows to emphasize the presence of a deeper information involved in the scaling indices $\tau = \tau(q, \gamma)$. And it turns out that the energy dependent mixing angle $\gamma = \gamma(E)$ might play there the role of an order parameter.

Numerical value of parameters entering the reformulated extended fundamental equation can be interpreted in terms of quantities describing the underlying self-similar process. Approach applied in the present paper does not bring into considerations, essentially, any free parameter.

It is shown that under certain conditions only one set of the scaling indices (from those describing intermittency and multifractality in terms of the G-moments) is sufficient to be considered because both sets are related.

Several stimulating suggestions are formulated in the present paper with the intention to draw attention of the experimental groups in looking for additional data (like intercepts and effective average multiplicity) which enter new relations governing the multifractal structures. Also the proposal is introduced to search for fractal structure when the partitioning in the (pseudo)rapidity (instead of the particle density) is performed. In general, to a better accuracy, experimental data on scaling indices characterizing the same type of collisions at more energies are wanted badly.

References

- [1] E.A. De Wolf, I.M. Dremin and W. Kittel: *Scaling Laws for Density Correlations and Fluctuations in Multiparticle Dynamics*. Preprint HEN-362 1993. To be published in Physics Reports.
- [2] A. Bialas and R. Peschanski: *Nucl. Physics B* **273** (1986), 703; and *ibid.*, 308 (1988) 857.
- [3] R.C. Hwa and J.C. Pan: *Phys. Rev. D* **45** (1992), 1476;
- [4] M. Blažek: *Czech. J. Phys.* **43** (1993), 111;
- [5] T.C. Halsey et al.: *Phys. Rev. A* **33** (1986), 1141;

- [6] M. Blažek: Multifractality and Phase Transitions at High Energies. In: *Hadron Structure '92*. Ed. by D. Bruncko and J. Urban, Inst. Exper. Physics SASci and Dept. Nucl. Physics, Šafárik University, Košice (1992), 82;
- [7] H. Satz: Nucl. Phys. B **326** (1989), 613;
- [8] A. Bialas and R.C. Hwa: Phys. Lett. **253** (1991), 436;
- [9] M. Blažek: Multifractals in High Energy Nuclear Collisions by Solving an Inverse Problem. In: *Quantum Inversion Theory and Applications*. Ed. by H.V. von Geramb, Springer Verlag, Berlin (1994), 389;
- [10] C. Amitrano, A. Coniglio and F. di Liberto: Phys. Rev. Lett. **57** (1986), 1016;
- [11] A. Martin: preprint CERN-TH 7093 (1993). ;
- [12] F. Rimondi, (CDF Collaboration), preprint FERMLAB-Conf-90/166-E, (1990) and to be published.
- [13] R. Peschanski: Nucl. Phys. B **327** (1989), 144;
- [14] P.L. Jain, G. Singh and A. Mukhopadhyay: Phys. Rev. C **46** (1992), 721;
- [15] M. Blažek: Fractal Structure in High Energy Nuclear Collisions. In: *Hadron Structure '93*. Ed. by S. Dubnicka and A.Z. Dubnicková, Inst. Physics of Slov. Acad. Sci., Bratislava (1993), 253;